

## A novel use of arterial spin labelling MRI to demonstrate focal hypoperfusion in individuals with posterior cortical atrophy: a multimodal imaging study

### INTRODUCTION

Posterior cortical atrophy (PCA) is a rare neurodegenerative syndrome, typically due to Alzheimer pathology, characterised by impairments in higher-order visual function and other parieto-occipital skills.<sup>1</sup> MRI measures of atrophy and <sup>18</sup>F-labelled fluorodeoxyglucose (FDG) positron emission tomography (PET) measures of glucose metabolism typically show posterior cortical deficits broadly mirroring the focal cognitive deficits.<sup>1</sup> By contrast, amyloid PET studies demonstrate

that fibrillar amyloid is widely deposited across the cortex.<sup>2</sup> Arterial spin labelling (ASL) is an MRI methodology that uses endogenous arterial blood water as a tracer to quantify cerebral blood flow (CBF).<sup>3</sup> We aimed to assess the ability of ASL to detect patterns of reduced CBF in PCA, and to compare these results with those from other imaging modalities.

### METHODS

Five patients fulfilling clinical diagnostic criteria for PCA,<sup>4</sup> and five controls attended for three scanning visits usually on consecutive days. On day 1, MRI scans were acquired on a 3 T Siemens TIM Trio scanner with a 32-channel phased array head-coil. Sequences included a sagittal three-dimensional (3D) MPRAGE T1-weighted volumetric scan (acquisition time 9 min 23 s, TE/TR/TI=2.9/2200/900 ms, dimensions 256×256×208, voxel size 1.1×1.1×1.1 mm), and coronal T2 fluid-attenuated inversion recovery (TE/TR/TI=87/9000/2500 ms, voxel size 0.9375×0.9375×5 mm). Perfusion data were acquired using pulsed ASL (FAIR Q2TIPS) with an 8-segment, background-suppressed 3D GRASE imaging readout<sup>5</sup> (acquisition time 6 min 40 s, T1/2=800/2000 ms, voxel size 3.8×3.8×4.0 mm, refocusing pulse flip angle 130°, five repetitions). A set of three saturation recovery images (TR=1,2,5 s) with the same readout module was also acquired to generate tissue M0 and T1 maps for CBF quantification. On day 2, each participant underwent a 10 min PET scan 50 min after an intravenous bolus of 300 MBq <sup>18</sup>F-florbetapir. On day 3, a 20 min PET scan was acquired 30–35 min postinjection of 185 MBq <sup>18</sup>F-FDG. PET scans were performed on a GE Discovery ST PET/CT scanner, with CT scans acquired immediately before each scan for attenuation correction.

T1-weighted images were processed using a Gaussian mixture model optimised through expectation maximisation to produce probabilistic segmentations of grey matter, white matter and cerebrospinal fluid. Regional labels were produced simultaneously from the integration of the template parcellations and the segmentation<sup>6</sup> to define (1) a reference region (whole cerebellum) for the PET normalisation; and (2) frontal, medial temporal, lateral temporal, parietal, posterior cingulate and occipital grey matter lobar regions which were subsequently corrected for total intracranial volume. ASL images were aligned to the T1-weighted image using a symmetric affine registration algorithm to reduce the

effects of any residual motion.<sup>7</sup> CBF maps were generated by fitting a derivative of the general kinetic model to the ASL data.<sup>8</sup> Florbetapir scans were rated amyloid-positive/negative on grey-scaled images according to standard guidelines; FDG scans were rated for regional hypometabolism. Standard uptake value ratios were calculated for each grey matter lobar region and as a composite, using whole cerebellum as the reference region.

Neuroimaging data from each patient were compared against the controls using a modified t test developed to conduct single participant comparisons, by treating the control sample as sample statistics rather than as population parameters.<sup>9</sup> To explore the regional relationships between the different techniques, z-scores for each modality and each lobe were calculated relative to controls, and linear regression was used across all brain regions to compare imaging modalities.

### RESULTS

Participant demographics and neuroimaging data are shown in online supplementary table S1. At the time of scanning, the patients (3 female, 2 male) had a mean  $\pm$ SD age of 59.4 $\pm$ 1.8 years. Single-participant images are shown in the figure 1, alongside the results from a control participant (male, 59 years old) as a reference. All patients were amyloid-positive, with fibrillar amyloid distributed widely across the cortex. Much more focal, posterior cortical reductions in cerebral blood flow, glucose metabolism and atrophy were seen. While atrophy in posterior regions was present in all patients, on visual assessment it was less pronounced than the metabolic deficits assessed using either FDG-PET or ASL.

Quantification of the regional results for each modality is shown in the online supplementary table S1. Compared with controls, there were consistent and significant reductions in grey matter volume and glucose metabolism in the parietal lobe in all patients, and in the parietal, occipital and lateral temporal lobes in the majority. Cerebral blood flow reductions were seen in the parietal and occipital lobes and posterior cingulate for all patients, reaching significance in three. In all cases amyloid deposition was distributed widely across the cortex, including the frontal lobes. Regression analyses showed no significant relationships between amyloid load and any other biomarker. There was no evidence for a relationship between grey matter volume and CBF ( $p=0.4$ ), borderline evidence for a relationship between grey matter volume and FDG-PET

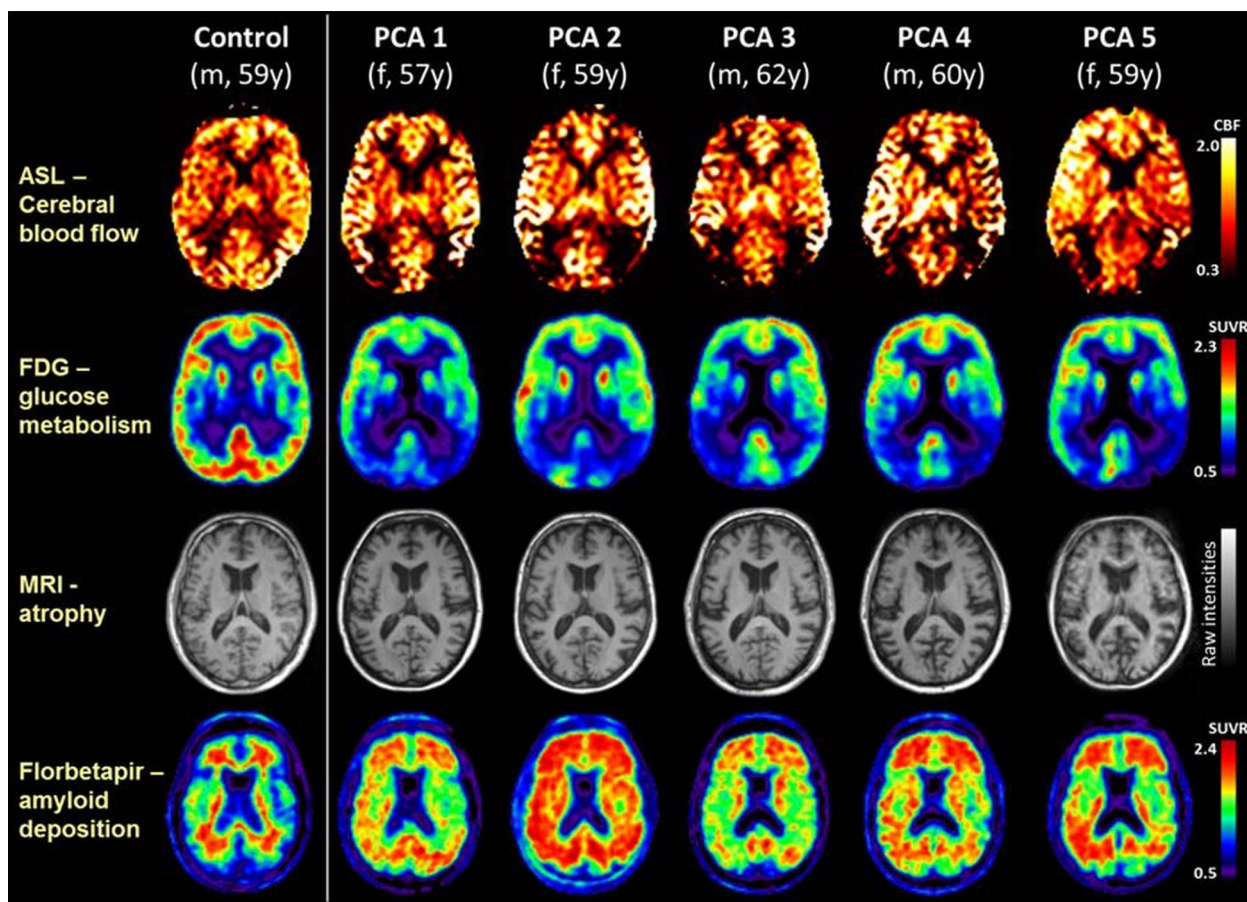


**Figure 1** Single-participant axial images for one control participant and five patients with PCA showing cerebral blood flow (ASL), glucose metabolism (FDG-PET), atrophy (structural MRI), and amyloid deposition (florbetapir-PET). For clinical purposes,  $^{18}\text{F}$ -florbetapir images should be read on a grey scale. ASL, arterial spin labelling; CBF, cerebral blood flow; FDG-PET,  $^{18}\text{F}$ -labelled fluorodeoxyglucose positron emission tomography; PCA, posterior cortical atrophy; SUVR, standard uptake value ratio.

metabolism ( $p=0.05$ ), but a significant correlation between regional CBF and FDG-PET metabolism ( $p=0.004$ ,  $R^2=0.26$ ).

## DISCUSSION

All individuals in this study had clinical and cognitive phenotypes consistent with PCA, and unequivocally positive florbetapir PET scans consistent with underlying AD pathology. In keeping with previous studies, amyloid deposition was widely distributed across the cortex<sup>2</sup> while atrophy, hypometabolism and CBF deficits were all more marked in posterior cortical regions.

Previous studies have shown correspondence between the pattern of cerebral hypometabolism measured using FDG-PET and ASL measures of CBF in typical late-onset AD<sup>10</sup> and semantic dementia.<sup>11</sup> Here, we extend these findings to PCA, but importantly show that these group level changes extend to individual patients. Posterior cortical CBF reduction was detectable in each of the individual patients with PCA and broadly

mirrored by the observed focal patterns of FDG-PET glucose hypometabolism—the gold standard for detecting regional metabolic changes. Both modalities exhibited more extensive changes than expected purely due to the posterior atrophy seen on structural imaging. These data show that ASL, a non-invasive MR sequence which can be implemented on standard clinical 3 T MR scanners, can usefully demonstrate CBF changes in individual patients with PCA. ASL may be a useful diagnostic adjunct in suspected PCA—and potentially other focal dementias—where an FDG-PET scan is unavailable.

Manja Lehmann,<sup>1</sup> Andrew Melbourne,<sup>2</sup> John C Dickson,<sup>3</sup> Rebekah M Ahmed,<sup>1</sup> Marc Modat,<sup>2</sup> M Jorge Cardoso,<sup>2</sup> David L Thomas,<sup>1,4</sup> Enrico De Vita,<sup>4,5</sup> Sebastian J Crutch,<sup>1</sup> Jason D Warren,<sup>1</sup> Colin J Mahoney,<sup>1</sup> Jamshed Bomanji,<sup>3</sup> Brian F Hutton,<sup>3</sup> Nick C Fox,<sup>1</sup> Xavier Golay,<sup>4</sup> Sebastien Ourselin,<sup>2</sup> Jonathan M Schott<sup>1</sup>

<sup>1</sup>Dementia Research Centre, UCL Institute of Neurology, London, UK

<sup>2</sup>Translational Imaging Group, Centre for Medical Image Computing, University College London, London, UK

<sup>3</sup>Institute of Nuclear Medicine, University College London Hospitals, London, UK

<sup>4</sup>Lysholm Department of Neuroradiology, National Hospital for Neurology and Neurosurgery, London, UK

<sup>5</sup>Neuroradiological Academic Unit, Brain Repair & Rehabilitation, UCL Institute of Neurology, London, UK

**Correspondence to** Dr Jonathan M Schott, Dementia Research Centre, UCL Institute of Neurology, 8-11 Queen Square, London WC1N 3BG, UK; [j.schott@ucl.ac.uk](mailto:j.schott@ucl.ac.uk)

**Acknowledgements** The authors acknowledge the support of the Leonard Wolfson Experimental Neurology Centre, the NIHR Queen Square Dementia Biomedical Research Unit and UCL/UCLH Biomedical Research Centre. The Dementia Research Centre is an Alzheimer's Research UK Co-ordinating Centre.

**Contributors** All the authors were responsible for drafting and revising the manuscript for content. ML, JCD, XG, SO, JMS were responsible for study concept and statistical analysis; ML, AM, JCD, MM, MJC, DLT, JB, BFH, JMS for analysis of the data; RMA, SJC, JDW, CJM, NCF, and JMS were responsible for patient recruitment; JCD, DLT, EDV for scan acquisition; and JMS for study supervision.

**Funding** AVID Radiopharmaceuticals (a wholly owned subsidiary of Eli Lilly), and the UK FTD Support Group.

**Competing interests** ML is supported by funding from Alzheimer's Research UK (ART-TRFUS2011-2). SC is supported by ESRC/NIHR (ES/K006711/1), EPSRC (EP/M006093/1) and an Alzheimer's Research UK

Senior Research Fellowship. SO is supported by the EPSRC (EP/H046410/1, EP/J020990/1, EP/K005278), the MRC (MR/J01107X/1), the EU-FP7 (FP7-ICT-2011-9-601055), the NIHR BRC UCLH/UCL HII (BW.mn. BRC10269). MM and DLT are supported by the UCL Leonard Wolfson Experimental Neurology Centre (PR/ylr/18575). JMS acknowledges the support of ARUK, the NIHR Biomedical Research Centre, Queen Square Dementia Biomedical Research Unit, and Medical Research Council.

**Patient consent** Obtained

**Ethics approval** Queen Square NRES Committee.

**Provenance and peer review** Not commissioned; externally peer reviewed.

► Additional material is published online only. To view please visit the journal online (<http://dx.doi.org/10.1136/jnnp-2015-312782>)



**OPEN ACCESS**

**Open Access** This is an Open Access article distributed in accordance with the terms of the Creative Commons Attribution (CC BY 4.0) license, which permits others to distribute, remix, adapt and build upon this work, for commercial use, provided the original work is properly cited. See: <http://creativecommons.org/licenses/by/4.0/>



CrossMark

**To cite** Lehmann M, Melbourne A, Dickson J C, *et al.* *J Neurol Neurosurg Psychiatry* 2016;**87**:1032–1034.

Received 25 November 2015

Accepted 27 November 2015

Published Online First 5 January 2016

*J Neurol Neurosurg Psychiatry* 2016;**87**:1032–1034.  
doi:10.1136/jnnp-2015-312782

**REFERENCES**

- 1 Crutch SJ, Lehmann M, Schott JM, *et al.* Posterior cortical atrophy. *Lancet Neurol* 2012;11:170–8.
- 2 Lehmann M, Ghosh PM, Madison C, *et al.* Diverging patterns of amyloid deposition and hypometabolism in clinical variants of probable Alzheimer’s disease. *Brain* 2013;136:844–58.
- 3 Haller S, Zaharchuk G, Thomas D, *et al.* Arterial spin label perfusion of the brain: emerging clinical applications. *Radiology* 2015;In Press.
- 4 Tang-Wai DF, Graff-Radford NR, Boeve BF, *et al.* Clinical, genetic, and neuropathologic characteristics of posterior cortical atrophy. *Neurology* 2004;63:1168–74.
- 5 Feinberg DA, Ramanna S, Guenther M. Evaluation of new ASL 3D GRASE sequences using parallel imaging, segmented and interleaved k-space at 3T with 12- and 32-channel coils. In: *Proceedings of the 17th Annual Meeting of ISMRM*. Honolulu, HI, USA; 2009:622.
- 6 Cardoso MJ, Modat M, Wolz R, *et al.* Geodesic information flows: spatially-variant graphs and their application to segmentation and fusion. *IEEE Trans Med Imaging* 2015;34:1976–88.
- 7 Modat M, Cash DM Daga P, *et al.* Global image registration using a symmetric block-matching approach. *J Med Imaging* 2014;1:024003.
- 8 Alsop DC, Detre JA, Golay X, *et al.* Recommended implementation of arterial spin-labeled perfusion MRI for clinical applications: a consensus of the ISMRM perfusion study group and the European consortium

- for ASL in dementia. *Magn Reson Med* 2015;73:102–16.
- 9 Crawford JR, Garthwaite PH. Investigation of the single case in neuropsychology: confidence limits on the abnormality of test scores and test score differences. *Neuropsychologia* 2002;40:1196–208.
- 10 Chen Y, Wolk DA, Reddin JS, *et al.* Voxel-level comparison of arterial spin-labeled perfusion MRI and FDG-PET in Alzheimer disease. *Neurology* 2011;77:1977–85.
- 11 Newberg AB, Wang J, Rao H, *et al.* Concurrent CBF and CMRGlc changes during human brain activation by combined fMRI-PET scanning. *Neuroimage* 2005;28:500–6.

**Supplementary Table:** Patient demographics and neuroimaging data

<b>Demographics</b>	<b>PCA 1</b>	<b>PCA 2</b>	<b>PCA 3</b>	<b>PCA 4</b>	<b>PCA 5</b>	<b>Controls (N=5) †</b>
<b>Age at time of scan, years</b>	57	59	62	60	59	63.9 (6.4)
<b>Gender</b>	F	F	M	M	F	2F, 3M
<b>Age at onset, years</b>	55	57	59	53	56	-
<b>Neuroimaging</b>						
<b>GM volume (% of TIV)</b>						
Frontal lobe	10.0%	9.3%	9.6%	10.7%	9.1%	10.8 % (0.7%)
Medial temporal lobe	2.0%	2.1%	2.2%	2.0%	1.7% *	2.2% (0.1%)
Lateral temporal lobe	5.1% *	5.0% *	5.5%	4.5% *	3.8% *	5.9% (0.2%)
Parietal lobe	4.7% *	4.8% *	4.3% *	4.4% *	4.6% *	6.3% (0.4%)
Posterior cingulate gyrus	0.4% *	0.4% *	0.4% *	0.5%	0.4% *	0.5% (0.03%)
Occipital lobe	4.4%	4.1%	4.4%	3.7% *	3.0% *	4.8% (0.5%)
<b>Cerebral blood flow (ml/100g/min)</b>						
Frontal lobe	35	32	29 *	35	48	39 (4)
Medial temporal lobe	31	30	35	28	38	28 (9)
Lateral temporal lobe	34	39	35	35	43	37 (7)
Parietal lobe	26	21 *	15 *	18 *	31	38 (7)
Posterior cingulate gyrus	35	26 *	30	27 *	36	43 (6)
Occipital lobe	24	28	16 *	16 *	26	41 (10)
Global mean	32	31	28	29	39	37 (8)
<b>FDG SUVRs</b>						
Frontal lobe	1.05	1.06	1.06	1.16	1.17	1.22 (0.09)
Medial temporal lobe	0.83 *	0.88	0.85	0.86	0.83 *	0.90 (0.03)
Lateral temporal lobe	0.92 *	1.00	0.93 *	0.88 *	0.88 *	1.12 (0.07)
Parietal lobe	0.84 *	0.91 *	0.79 *	0.80 *	0.84 *	1.22 (0.11)
Posterior cingulate gyrus	0.95 *	0.83 *	1.06 *	1.02 *	0.97 *	1.32 (0.12)
Occipital lobe	0.91 *	1.16	0.89 *	0.85 *	0.73 *	1.19 (0.08)
Global mean	0.94	1.00	0.94	0.96	0.93	1.13 (0.13)
<b>AV45 SUVR</b>						
Frontal lobe	1.38	1.68 *	1.41	1.48 *	1.35	1.06 (0.16)
Medial temporal lobe	1.12 *	1.27 *	1.10	1.18 *	1.07	0.95 (0.07)
Lateral temporal lobe	1.41 *	1.68 *	1.36 *	1.41 *	1.35 *	1.02 (0.09)
Parietal lobe	1.41 *	1.63 *	1.35 *	1.41 *	1.31	1.07 (0.12)
Posterior cingulate gyrus	1.53 *	1.65 *	1.48 *	1.45 *	1.23	1.03 (0.10)
Occipital lobe	1.48 *	1.49 *	1.19	1.45 *	1.42	1.09 (0.15)
Global mean	1.38 *	1.57 *	1.33 *	1.40 *	1.30 *	1.03 (0.11)

\* significantly different from control values ( $p < 0.05$ ); † Mean (SD) of 5 control subjects, TIV – Total Intracranial Volume